

Interaction processes between dislocations and particles in the ODS nickel-base superalloy INCONEL MA 754 studied by means of in situ straining in an HVEM

D. Häussler^a, B. Reppich^a, M. Bartsch^b, U. Messerschmidt^{b,*}

^a Institute for Materials Science I, University of Erlangen-Nuremberg, Martensstraße 5, D-91058 Erlangen, Germany

^b Max Planck Institute of Microstructure Physics, Weinberg 2, D-06120 Halle (Saale), Germany

Abstract

In situ straining experiments in a high-voltage electron microscope (HVEM) have been performed on the oxide-dispersion strengthened (ODS) nickel-base superalloy INCONEL MA 754 at 1020 and 1065 K. The results can be interpreted by interfacial pinning of dislocations at the dispersoids and, in some cases, by the Orowan mechanism. In addition to the thermally activated detachment of dislocations from particles, a viscous friction mechanism possibly due to point defect diffusion in the dislocation cores and Taylor hardening contribute to the flow stress. © 2001 Elsevier Science B.V. All rights reserved.

Keywords: Plastic deformation; Oxide dispersion strengthening; Dislocation dynamics; Electron microscopy

1. Introduction

It was the aim of this work to investigate the way moving dislocations are impeded by dispersoids that are added to a nickel-base superalloy in order to improve its creep resistance. INCONEL MA 754¹ has been chosen not only because of an interest in this material but also because it is a suitable model material. Although materials of this class were introduced decades ago and the technology is widely controlled, a comprehensive understanding of the action of dispersoids is still missing. Meanwhile, the dislocation theory of particle strengthening has attained a high level, e.g. [1]. To the classical interaction models an additional one was introduced in the eighties — the attractive interaction between the dislocations and particles, known as interfacial pinning [2]. According to this model, the dislocations pass the dispersoids by climb and get pinned at their departure sides. The rate-controlling step is the thermally activated detachment from the pinned configurations [3,4]. The theory has further been improved, e.g. in [5]. According to the theory, the dislocations spend most of their time at the departure side of the dispersoids. To prove such a behaviour, in situ straining experiments in a high-voltage electron microscope are especially valuable. In spite of first in situ experiments on other materials [6,7], many problems are still open.

* Corresponding author. Tel.: +49-345-5582927; fax: +49-345-5511223.
E-mail address: um@mpi-halle.mpg.de (U. Messerschmidt).

¹ Trademark of Inco Alloys International Ltd.

2. Experimental

INCONEL MA 754 with the composition NiCr(20 wt.%)–Al(0.3)Ti(0.5)Fe(1.0)C(0.05)Y₂O₃(0.6) contains stable Y₂Ti₂O₇ oxide particles at a volume fraction of $f = 1.1\%$, an average diameter of $d = 13.6$ nm, and a mean particle spacing in the slip plane of $L = 94$ nm [8,9]. The specimen areas investigated here may always be regarded as parts of a single crystal because of the coarse-grained structure with the tensile axis being close to [0 1 0] and the foil normal close to [1 0 1], respectively.

The microtensile specimens were prepared by cutting slices of about 8 mm × 2 mm × 0.1 mm and electrolytic jet polishing. They were fixed to the grips of the tensile stage [10] of a high-voltage electron microscope operated at 1 MV. The in situ straining experiments were performed at 1020 and 1065 K. In contrast to higher temperatures, the specimens degraded only negligibly. Video recordings were taken of moving dislocations. No differences were observed between the dislocation behaviour at the two temperatures.

3. Results

The slip plane of dislocations with $a/2\langle 110 \rangle$ Burgers vector is $\{111\}$. For the [0 1 0] tensile axis applied to the specimen, which causes an almost uniaxial stress in the same direction near the side edges of the perforation, there are eight equivalent slip systems of orientation factors of

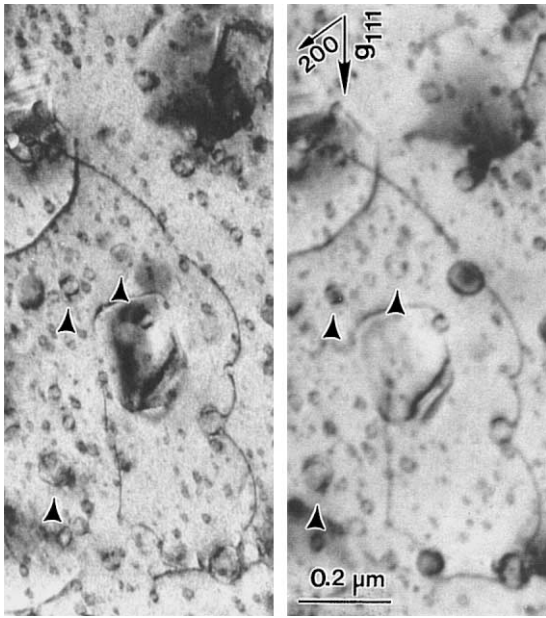


Fig. 1. Stereo pair of the microstructure obtained after an in situ straining experiment at 1020 K taken in the unloaded state at room temperature.

$m = 0.41$. Almost all Burgers vectors may occur except $a/2[101]$ and $a/2[10\bar{1}]$, which are perpendicular to the tensile axis. The shapes of dislocation segments bowing out under stress have been calculated in the framework of the line tension model in anisotropic elasticity [11].

After the in situ experiments, many particles are decorated by rings of weak dark uniform contrast. Some of them are labelled in Fig. 1. These contrasts may belong to Orowan loops which are created around the particles by the moving dislocations. During the in situ experiments, where optimum imaging conditions cannot always be achieved, the dark contrasts around the particles became more prominent. Special contrast experiments have been performed to de-

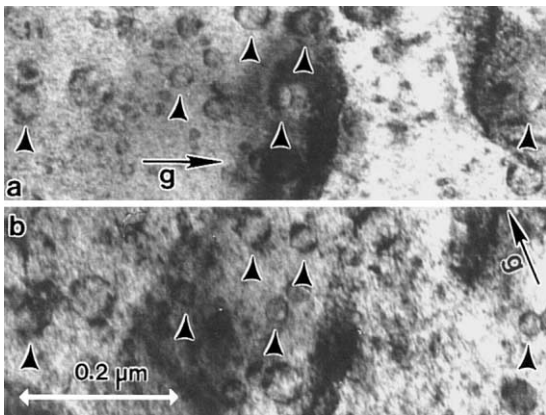


Fig. 2. Microstructure after an in situ straining experiment at 1020 K at different \vec{g} vectors. Examples for ring-shaped contrasts marked by arrowheads. (a) $\vec{g} = [11\bar{1}]$ and (b) $[\bar{1}11]$.

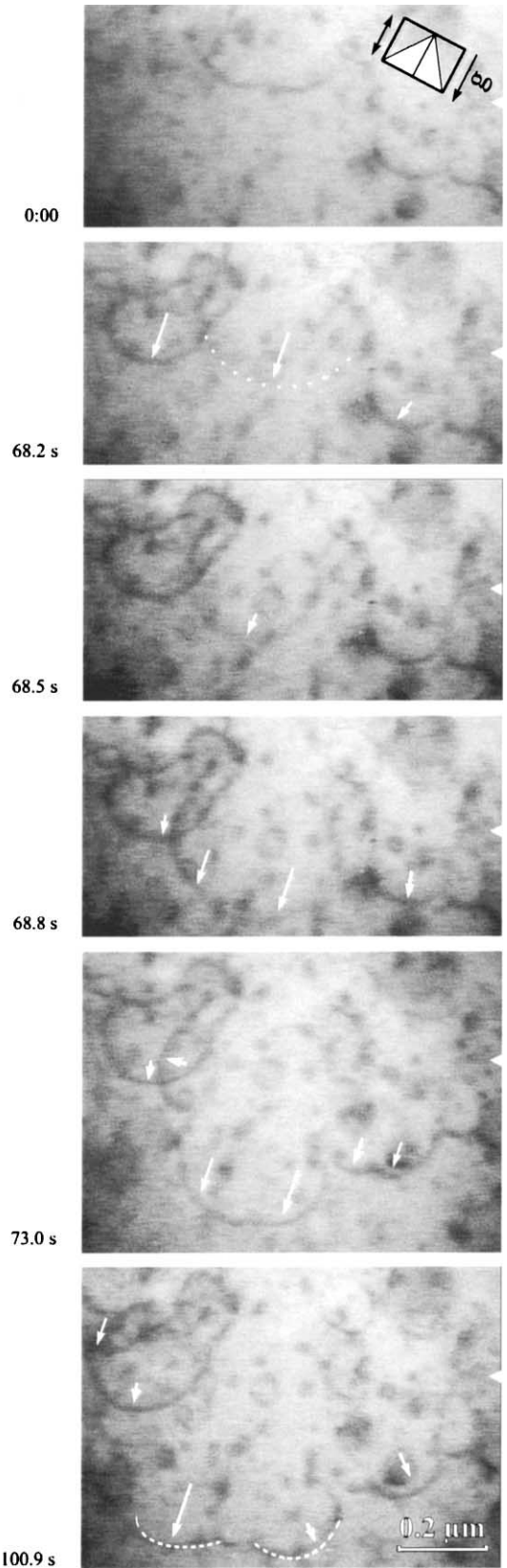


Fig. 3. Video record of the movement of dislocations through an oxide particle array observed at 1020 K. Frames two to four were taken after very short time intervals. After the last frame the marked dislocation had detached from the pinned configuration immediately.

termine the nature of these contrasts. If they were Orowan loops, the contrast should be extinguished at the same vectors which extinguish the dislocations. Using the $\langle 111 \rangle$ type diffraction vectors of Fig. 2a and b, the contrast of loops should be extinguished either on Fig. 2a or Fig. 2b. The figures demonstrate that most contrast rings appear on both micrographs. Thus, the contrasts cannot unequivocally be attributed to pure Orowan loops of the active slip systems. A complicated strain field of the particles may cause these contrasts. Besides, the formation of Orowan loops could not directly be proved by a respective video sequence. Consequently, the contrast rings might appear as a result of the thermal treatment or some radiation damage during the in situ experiments.

The dynamic behaviour of dislocations interacting with the particles is observed from the video records. It depends on the local strain rate. Two cases may be distinguished.

Firstly, if the strain rate is low, most dislocations rest at obstacles for an essential part of the total time, e.g. in Fig. 3. This series is a representative one, because of the size of the observed area and the duration of the observation. However, a sequence of a few frames cannot represent all details of the dislocation movement. Relatively stable positions are attained at 0.00 and 73.0 s, in contrast to rapidly changing situations in the remaining frames of the figure. Arrows mark

changes. In the second frame at 68.2 s, the contrast of the quickly moving central segment is so weak that it is almost invisible, but its position is marked. Thus, the movement of the dislocations is quite jerky on a mesoscopic scale, and together with other experimental results not shown here, can be described in the following way. After an obstacle is overcome, the formerly pinned segment may move under the strong self stress of the backward cusp at a very high velocity, which frequently cannot be resolved by the video recording. Afterwards, the dislocation segment moves viscously until it touches the next particle.

Due to the increasing of self stress, which counteracts the applied stress, the dislocation segments adjoining the particle bow out slowly. At low dislocation velocities, the time observed for bowing is less than that for waiting for detachment from the pinned equilibrium configurations. The angles of attack range typically between about 30° and 85° .

Secondly, at higher local deformation rates (Fig. 4), which are usually connected with a higher density of moving dislocations, the dislocations do not spend most of their time waiting at the obstacles. Thus, the dislocation motion is much less jerky. The times necessary for bowing out may be larger than those for detachment. Frequently, many dislocations move simultaneously. In these cases, they may move in a collective way, suggesting that long-range interactions are

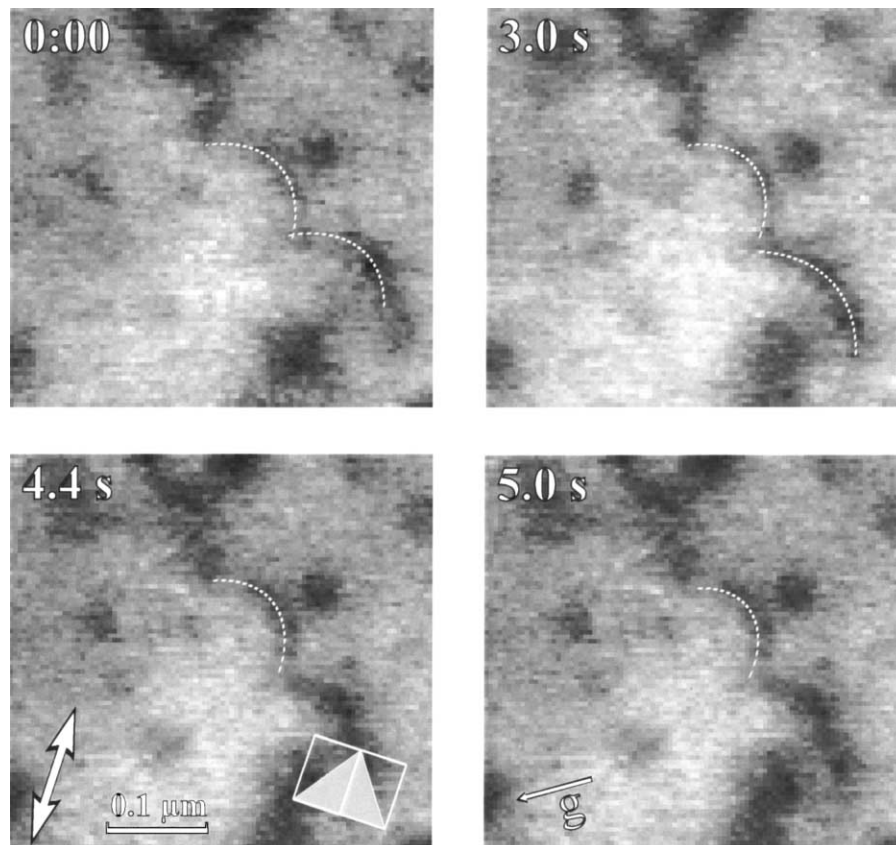


Fig. 4. Video sequence of four different dislocations being pinned consecutively at the same array of oxide particles at 1020 K.

also important. The mean angles of attack at the obstacles are frequently larger than 90° .

Information on the effective density of the interacting particles on the slip plane can be obtained from the obstacle spacing l , i.e. the average value of the distances between the obstacles along the dislocation lines in the pinned configurations. It can be measured directly from the video tapes as the distance between the cusps formed at the obstacles. The evaluation yields $l \approx 150$ nm. This value can be compared with so-called Friedel spacing l_F calculated with the mean planar lattice spacing $L = 94$ nm [9], determined from conventional transmission electron microscopy according to $l_F = L/[\sin(\theta/2)]^{1/2}$ [1]. Using $\theta = 30\text{--}85^\circ$ (see above), one obtains $l_F = 120\text{--}190$ nm comprising the experimental value of l .

Bowed-out dislocation segments cause a back stress τ_b , which is superimposed on the locally acting stress. If the dislocation segments are in elastic equilibrium, both stresses balance each other so that the local stress can be evaluated from the curvature of the bowed-out dislocation segments, as it is reviewed in [12]. For this aim, the shape of bowed-out segments was calculated in the framework of the line tension model using elastic anisotropy [11]. Accordingly, the back stress is given by

$$\tau_b = \frac{E_s}{by_0} \ln \left(\frac{l}{5b} \right) \quad (1)$$

where E_s is the pre-logarithmic factor of the line energy of a screw dislocation, b the magnitude of the Burgers vector, and y_0 the minor half axis of the dislocation loops. As the elastic constants of INCONEL MA 754 were not available, the values of pure Ni, which is the main constituent of the alloy, for room temperature were used [13]. With $b = 0.249$ nm there follows $E_s = 3.88 \times 10^{-10}$ N. To take into account the high temperature of the experiments, we use a slightly smaller value of $E_s = 3.7 \times 10^{-10}$ N. The respective shape of dislocation loops in equilibrium is inserted into Figs. 3 and 4. In order to determine the size values y_0 of actual bowed-out segments in stable positions, loops in an appropriate projection were scaled until they match the experimental segments. Since the directions of Burgers vectors were not known, the loop orientation was chosen which fitted best the ellipticity of the experimental segments. Values of the back stress were calculated by Eq. (1) using the individual lengths l of the segments. The average value of 16 representative segments is $\tau_b = 91$ MPa.

In some cases, calculated dislocation segments on $\{111\}$ planes did not fit to the experimental segments. Besides, in stereo pairs like Fig. 1 (taken in the relaxed state), the segments bowing out between dispersoids do not lie on any of the $\{111\}$ planes. In this particular case, the bowing may result from residual stresses. Nevertheless, sometimes dislocations were observed which have left their original slip planes during straining at high temperatures.

4. Discussion

The present experiments give some evidence that the motion of the dislocations is not confined to single $\{111\}$ planes. The dislocations cross slip and move also on other planes or even climb.

The in situ experiments yield clear evidence that the dislocation motion in INCONEL MA 754 is impeded by the presence of the oxide dispersoids. At low temperatures, the incoherent particles have to be bypassed by the Orowan process. Although during in situ deformation at high temperatures loop contrasts appear at many particles, Fig. 2 does not prove them to be Orowan loops. On the other hand, large particles seem to be wrapped by Orowan loops, which is not shown in this paper. The conclusion may be that the dislocations are pinned at the majority of particles by the interfacial pinning mechanism [2–4]. This is corroborated by the fact that at low stresses the dislocations spend an appreciable time between being fully bowed-out and detachment. Since the Orowan process is of athermal nature, the particles should be surmounted immediately after the dislocations being fully bowed-out.

The experimentally observed back stress $\tau_b = 91$ MPa proves to be significantly lower than the theoretical values of the Orowan stress τ_{OR} , which is according to [14]

$$\tau_{OR} = \frac{2E}{b(l-d)} \left\{ \ln \left[\frac{d(1-d/l)}{b} \right] + 0.7 \right\} \quad (2)$$

where for the screw dislocation E is the pre-logarithmic factor of the energy of an edge dislocation, and vice versa. With the energy factors for screw dislocations $E_s = 3.7 \times 10^{-10}$ N and for edge dislocations $E_e = 5.78 \times 10^{-10}$ N, $l = 150$ nm and the particle diameter $d = 13.6$ nm from Sections 2 and 3, the Orowan stresses of screw and edge dislocations are $\tau_{OR}^s = 157$ MPa and $\tau_{OR}^e = 100$ MPa.

The back stress can also be compared to the contribution of the particles to the flow stress determined from a comparison between the creep data of INCONEL MA 754 and the particle-free reference material Nimonic 75 [8,9]. This contribution amounts to 180–205 MPa, depending on the strain rate $\dot{\epsilon}$, which corresponds to $\tau_{part} = 70\text{--}80$ MPa after transformation to a shear stress. These values were estimated for a slightly higher temperature (1123 K), which may explain the deviation. In conclusion, the considerable values of the back stress characterize the particles as relatively strong obstacles, even at high temperatures where the dislocations can bypass them by climb and subsequently detach from the obstacles by thermal activation.

The viscous motion of the dislocations between the particles at high temperatures suggests that their velocity is controlled by a diffusive friction mechanism, as concluded previously from the in situ deformation study on INCOLOY MA 956 [7], presumably the Cottrell mechanism, either from the Cr but more probably from the trace elements in the alloy. The viscous friction mechanism may explain the different dynamic behaviour of dislocations in the matrix, in

front of and, in particular, behind dispersoids at low or high deformation rates (unpublished research).

The collective motion of dislocations, which was observed at higher local deformation rates, is certainly due to mutual long-range dislocation interactions. They cause a further important contribution to the flow stress owing to Taylor hardening, which has been estimated to $\tau_G \approx 86$ MPa (unpublished research), close to values quoted from creep data [9].

5. Conclusions

The flow stress of INCONEL MA 754 at high temperatures may consist of three major contributions, the stress for thermally activated detachment from the oxide particles, which should be equal to the back stress $\tau_b \approx 91$ MPa, a viscous friction stress owing to point defect diffusion processes in the dislocation cores, which is important particularly at high dislocation velocities but cannot be estimated from the present experiments, and a long-range contribution $\tau_G \approx 86$ MPa.

Acknowledgements

The authors are grateful to Bernhard Kummer, Christian Dietzsch and Wolfgang Greie for technical help. They

thank the Deutsche Forschungsgemeinschaft for financial support.

References

- [1] B. Reppich, in: H. Mughrabi (Ed.), *Materials Science and Technology*, Vol. 6, VCH-Weinheim, New York, Basel, Cambridge, 1993, p. 321.
- [2] D.J. Srolovitz, M.J. Luton, R.A. Petkovic-Luton, D.M. Barnett, W.D. Nix, *Acta Metall.* 32 (1984) 1079.
- [3] E. Arzt, J. Rösler, *Acta Metall.* 36 (1988) 1053.
- [4] J. Rösler, E. Arzt, *Acta Metall.* 38 (1990) 671.
- [5] B. Reppich, *Acta Mater.* 46 (1998) 61.
- [6] R. Behr, J. Mayer, E. Arzt, *Intermetallics* 7 (1999) 423.
- [7] M. Bartsch, A. Wasilkowska, A. Czyska-Filemonowicz, U. Messerschmidt, *Mater. Sci. Eng. A* 272 (1999) 152.
- [8] M. Heilmaier, K. Wetzel, J. Wunder, B. Reppich, in: H. Oikawa, et al. (Eds.), *Strength of Materials*, Jpn. Inst. Met., 1994, p. 567.
- [9] M. Heilmaier, J. Wunder, U. Böhm, B. Reppich, *Comput. Mater. Sci.* 7 (1996) 159.
- [10] U. Messerschmidt, M. Bartsch, *Ultramicroscopy* 56 (1994) 163.
- [11] D. Baither, University of Munster PC programme for calculating line tension data in anisotropic elasticity.
- [12] U. Messerschmidt, *Z. Metallkde.* 84 (1993) 391.
- [13] J.P. Hirth, J. Lothe, *Theory of Dislocations*, Wiley, New York, 1982.
- [14] D.J. Bacon, U.F. Kocks, R.O.S. Scattergood, *Philos. Mag.* 26 (1973) 1241.